

Experimental macroscopic coherence by phase-covariant cloning of a single photon

Eleonora Nagali¹, Tiziano De Angelis¹, Fabio Sciarrino^{2,1}, and Francesco De Martini¹

¹Dipartimento di Fisica dell'Università "La Sapienza" and Consorzio

Nazionale Interuniversitario per le Scienze Fisiche della Materia, Roma, 00185 Italy

²Centro di Studi e Ricerche "Enrico Fermi", Via Panisperna 89/A, Compendio del Viminale, Roma 00184, Italy

We investigate the multiphoton states generated by high-gain optical parametric amplification of a single injected photon, polarization encoded as a "qubit". The experiment configuration exploits the optimal phase-covariant cloning in the high gain regime. The interference fringe pattern showing the non local transfer of coherence between the injected qubit and the mesoscopic amplified output field involving up to 4000 photons has been investigated. A probabilistic new method to extract full information about the multiparticle output wavefunction has been implemented.

PACS: 03.67.-a, 03.67.Hk, 42.65.Lm

PACS numbers:

The problem of manipulating and controlling the flux of quantum information from a quantum system to many ones has been generally tackled and solved by the theory of quantum cloning [1, 2, 3]. Indeed, from a practical point of view, this process is considered a useful tool for the optimal distribution of quantum information carried by N qubits into several quantum channels and for the transmission of information contained in a system into correlations between many systems. On a more fundamental level, it has been suggested that, in the domain of quantum optics, the cloning process can also be adopted to investigate the intriguing transition of the quantum behavior from the "microscopic world", represented here by one of few properly encoded photons, to the mesoscopic and macroscopic one composed by many particles [4, 6].

In quantum optics, the qubit is generally implemented by exploiting the polarization state $\vec{\pi}$ of a single photon. It is there natural to associate a cloning map with the process of stimulated emission [7]. In the present framework, the quantum injected - optical parametric amplifier (QI-OPA), which exploits the process of stimulated emission in a nonlinear (NL) crystal, has led to the experimental realization of the 1 to 2 cloning machine in different configurations [8, 9, 10]. Recently, the coherence-preserving character of high-gain OPA allowed the reproduction of the quantum superposition condition of an input single-particle qubit $\alpha|H\rangle + \beta|V\rangle$, where $|H\rangle$ and $|V\rangle$ are respectively single photon state of horizontal ($\vec{\pi}_H$) and vertical ($\vec{\pi}_V$) polarization, in a multi-particle amplified output field involving an average of $\simeq 6$ clones [11]. The adoption of more powerful amplifier operating at the quantum level could open new perspectives for the generation of unique quantum states for the implementation of new tests of fundamental physics and innovative protocols for quantum metrology [12].

The present work reports the optical parametric amplification of a single photon in the high gain regime to experimentally investigate how the information initially

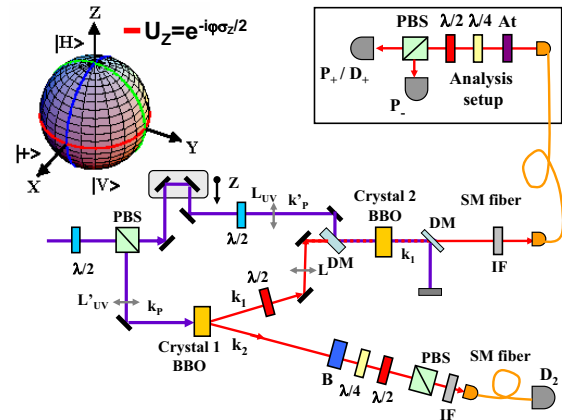


FIG. 1: Optical configuration of the quantum injected optical parametric amplifier. The SPDC quantum injector (crystal 1) is provided by a type II generator of polarization entangled photon couples. Crystal 2, realizing the OPA action, is cut for collinear type II phase matching. Both crystals are 1.5 mm thick. The fields are coupled to single mode (SM) fiber. The UV beam was focused on crystal 2 with L'_{UV} (focal length = 30 cm). Bloch sphere representation of the input qubit.

contained in its polarization state is distributed over a large number of particles. In particular we analyze how the coherence properties of the input state are transferred to the mesoscopic output field. Fringe patterns have been observed for output fields involving up to 4×10^3 photons.

The adopted QI-OPA configuration is the highly efficient collinear regime [13], which generates pairs of photons over the same output spatial mode \mathbf{k}_1 . This transformation realizes the optimal distribution of quantum information for qubits restricted to a subspace of the polarization space [14]. Specifically, here we consider the optimal process for equatorial qubit of the corresponding Bloch sphere: $|\varphi\rangle = 2^{-1/2}(|H\rangle + e^{i\varphi}|V\rangle)$ (Fig.1); since the information is codified in the phase φ of the input qubit, the process is called phase-covariant cloning

[15, 16]. The partial a-priori information on the qubit to be cloned leads to a high visibility coherence of the generated multiphoton superposition.

The experimental layout is sketched in Figure 1. The excitation source is a Ti:Sa Coherent MIRA mode-locked laser further amplified by a Ti:Sa regenerative REGA device operating with pulse duration $180fs$ at a repetition rate of $100kHz$ with average output power equal to $720mW$. The output beam, frequency-doubled by second harmonic generation, provides the excitation beam of UV wavelength (wl) $\lambda_P = 397.5nm$ and power $300mW$. The UV beam is splitted in two beams through a $\lambda/2$ waveplate and a polarizing beam splitter (PBS) and excites two BBO (β -barium borate) NL crystals cut for type II phase-matching. Crystal 1, excited by the beam \mathbf{k}_P , is the spontaneous parametric down-conversion (SPDC) source of entangled photon couples of wl $\lambda = 2\lambda_P$, emitted over the two output modes \mathbf{k}_i ($i = 1, 2$) in the *singlet* state $|\Psi^-\rangle_{k_1, k_2} = 2^{-\frac{1}{2}}(|H\rangle_{k_1}|V\rangle_{k_2} - |V\rangle_{k_1}|H\rangle_{k_2})$. The pump power of beam \mathbf{k}_P is set in order to have a negligible probability to generate two pairs of photons. While the photon associated to mode \mathbf{k}_2 is coupled into a single mode fiber and excites the single photon counting module (SPCM) D_2 (hereafter referred to as *trigger* mode), the single photon state generated over the mode \mathbf{k}_1 is injected, together with an UV pump beam (mode \mathbf{k}'_P), into the non-linear crystal 2 and stimulates the emission of many photon pairs. By virtue of the nonlocal correlation acting on modes \mathbf{k}_1 and \mathbf{k}_2 , the input qubit on mode \mathbf{k}_1 is prepared in the state $|\varphi\rangle_{k_1} = 2^{-\frac{1}{2}}(|H\rangle_{k_1} + e^{i\varphi}|V\rangle_{k_1})$ by measuring the photon on mode \mathbf{k}_2 in the appropriate polarization basis. This measurement is carried out by adopting a set $\lambda/2 + \lambda/4$ waveplates, a phase shifter (B) and a polarizing beam-splitter PBS . By an adjustable spatial delay (Z), the time superposition in the OPA of the excitation UV pulse and of the injection photon wavepacket is ensured. The injected single photon and the UV pump beam \mathbf{k}'_P are superposed exploiting a dichroic mirror (DM) with high reflectivity at λ_P and high transmittivity at λ .

The crystal 2 is oriented for collinear operation over the two linear polarization modes, respectively horizontal and vertical. The interaction Hamiltonian of the optical parametric amplification (crystal 2) $\hat{H} = i\chi\hbar(\hat{a}_H^\dagger\hat{a}_V^\dagger) + h.c.$ acts on the single spatial mode \mathbf{k}_1 where \hat{a}_π^\dagger is the one photon creation operator associated to \mathbf{k}_1 mode with a polarization $\vec{\pi}$. The main feature of this Hamiltonian is its peculiar property of phase-covariance for qubits with equatorial polarization, leading to the optimality of the cloning process. Owing to this invariance under $U(1)$ transformations, we can then re-write: $\hat{H} = \frac{1}{2}i\chi\hbar e^{-i\varphi}(\hat{a}_\varphi^{\dagger 2} - e^{i2\varphi}\hat{a}_{\varphi\perp}^{\dagger 2}) + h.c.$ for $\varphi \in (0, 2\pi)$ where $\hat{a}_\varphi^\dagger = 2^{-1/2}(\hat{a}_H^\dagger + e^{i\varphi}\hat{a}_V^\dagger)$ and $\hat{a}_{\varphi\perp}^\dagger = 2^{-1/2}(-e^{-i\varphi}\hat{a}_H^\dagger + \hat{a}_V^\dagger)$. Any injected state $|\varphi\rangle_{k_1}$ on mode

\mathbf{k}_1 evolves into the output state $|\Phi\rangle_{k_1}^\psi = \hat{U}|\varphi\rangle_{k_1}$ according to the OPA unitary $\hat{U} = \exp[-i\hat{H}t/\hbar]$, being t the interaction time [10]. In particular we shall consider the action over states with polarization $\vec{\pi}_\pm = 2^{-\frac{1}{2}}(\vec{\pi}_H \pm \vec{\pi}_V)$. The overall output state amplified by the OPA apparatus is found to be expressed as:

$$\begin{aligned} |\Sigma\rangle_{k_1, k_2} &= (\hat{U} \otimes \hat{1}) |\Psi^-\rangle_{k_1, k_2} = \\ &= 2^{-1/2} \left(|\Phi\rangle_{k_1}^+ |-\rangle_{k_2} - |\Phi\rangle_{k_1}^- |+\rangle_{k_2} \right) \end{aligned} \quad (1)$$

with

$$|\Phi\rangle_\pm = \frac{|\Phi\rangle^H \pm |\Phi\rangle^V}{\sqrt{2}} = \sum_{i,j=0}^{\infty} \gamma_{ij} \frac{\sqrt{(1+2i)!(2j)!}}{i!j!} |2i+1\rangle_\pm |2j\rangle_\mp \quad (2)$$

and $\gamma_{ij} \equiv C^{-2}(-\frac{\Gamma}{2})^i (\frac{\Gamma}{2})^j$, $C \equiv \cosh g$, $\Gamma \equiv \tanh g$, being g the NL gain [8]. There $|p\rangle_+ |q\rangle_-$ stands for a state with p photons with polarization $\vec{\pi}_+$ and q photons with $\vec{\pi}_-$. The multi-particle states $|\Phi\rangle^+$, $|\Phi\rangle^-$ are orthonormal, i.e. $\langle\Phi|\Phi\rangle^j = \delta_{ij}$. Similar expressions holds for any equatorial pair of polarizations $\{\vec{\pi}_\varphi, \vec{\pi}_{\varphi\perp}\}$ due to the phase-covariance of the overall process: $|\Phi\rangle^\varphi = 2^{-1/2}(|\Phi\rangle^H + e^{i\varphi}|\Phi\rangle^V)$. Note that the state $|\Sigma\rangle_{k_1, k_2}$, generally dubbed "Schroedinger Cat State" keeps its *singlet* character in the multi-particle regime, and expresses the nonlocal correlations between two distant objects: the *microscopic* (single particle) system expressed by the *trigger* state (mode \mathbf{k}_2) and the *mesoscopic* (multiparticle) system (\mathbf{k}_1) [17, 18].

Let us analyze the output field \mathbf{k}_1 over the polarization modes $\vec{\pi}_\pm$ when the state $|\varphi\rangle_{k_1}$ is injected. The average photon number N_\pm over \mathbf{k}_1 with $\vec{\pi}_\pm$ is found to depend on the phase φ as follows: $N_\pm(\varphi) = \bar{m} + \frac{1}{2}(2\bar{m} + 1)(1 \pm \cos \varphi)$ with $\bar{m} = \sinh^2 g$. The conditions $\varphi = 0$ and $\varphi = \pi$ correspond to single-photon injection and no-injection of the mode $\vec{\pi}_+$, respectively. The average photon number related to both cases is: $N_+(0) = 3\bar{m} + 1$ and $N_+(\pi) = \bar{m}$. For $\varphi = 0$, the average number of photons emitted over the two polarizations over \mathbf{k}_1 is found to be $M = 4\bar{m} + 1$. We conclude that the output state with polarization $\vec{\pi}_\pm$ exhibits a sinusoidal fringe pattern of the field intensity depending on φ with a gain-dependent visibility $\mathcal{V}^{th} = \frac{2\bar{m}+1}{4\bar{m}+1}$ [13]. Note that for $g \rightarrow \infty$, viz. $M \rightarrow \infty$ the fringe visibility of this 1st - order correlation function attains the asymptotic values $\mathcal{V}^{th} = 50\%$.

The output field emerging from the crystal 2 with wl λ was filtered against the UV pump beam by a dichroic mirror and by an interferential filter (IF) with bandwidth equal to $1.5nm$. It was then coupled to a single mode fiber, polarization analyzed and then detected by the photomultipliers tubes (P_+ and P_-). These were Burle A02 10-dynode detectors with a Ga-As photocathode having $\eta_{QE} = 13\%$. The signals were registered by a fast digital oscilloscope [Tektronix TDS5104D] triggered by D_2 .

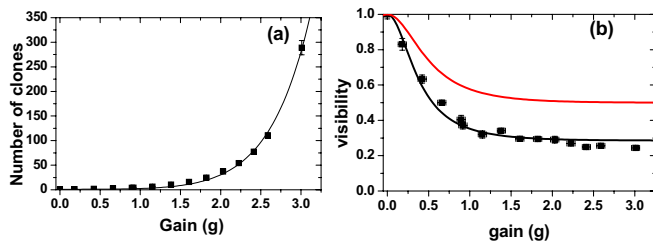


FIG. 2: (a) Number of clones versus the non-linear gain. Black curve: best fit; (b) Visibility of the fringe patterns versus the gain value rescaled by \mathcal{V}^{in} . Solid line: $\tilde{\mathcal{V}}^{th}$ with and $p = 0.4$; dashed line: \mathcal{V}^{nc} ; dotted line \mathcal{V}^{th} .

In a first experiment the gain value g of the optical parametric process and the overall quantum efficiency of the detection apparatus were measured in absence of quantum injection. We obtained $g_{max} = (4.34 \pm 0.02)$, while the overall detection efficiency η_1 on the \mathbf{k}_1 mode was estimated $\eta_1 \simeq 1.6\%$. The latter one was contributed by the fiber coupling ($\sim 50\%$), IF transmittivity ($\sim 25\%$) and detector's quantum efficiency (η_{QE}). By setting $g = 0$ the effective visibility of the input qubit was measured: $\mathcal{V}_{in} = (78.4 \pm 5.1)\%$, a result attributed to double-pairs emission from crystal 1. By subtracting these accidental coincidences the input qubit visibility was raised to $(96.5 \pm 2.5)\%$.

In order to investigate how the coherence of the input qubit survives to the amplification process, we measured the fringe pattern visibilities of the output field for different values of the gain value of the OPA. The interference property of the output field implied by the quantum superposition character of the input qubit $|\varphi\rangle_{k_1}$ was measured in the basis $\vec{\pi}_{\pm}$ over the output "cloning" mode \mathbf{k}_1 by signals of P_+ and P_- conditioned by the detection of a single photon from D_2 for different phases of the injected qubit. Figure 2 reports the gain dependence of the number of clones rescaled by the visibility of the input qubit \mathcal{V}_{in} . The solid line reports the best fit curve with a theoretical model $\tilde{\mathcal{V}}^{th}$ which incorporates the main experimental imperfections: $\tilde{\mathcal{V}}^{th} = \frac{p(2\overline{m}+1)}{p(2\overline{m}+1)+2\overline{m}}$. There the parameter p represents the probability that the injected heralded photon over the detected modes gives rise to stimulated emission. It differs from 1 because of the partial mismatches between the amplifying pump beam and the input single photon state. By fitting the experimental data we found $p=0.40 \pm 0.01$ (Fig.3-b), which is in agreement with a theoretical estimation obtained by the expression $p \simeq T \times \Delta\nu \times \Delta k$ where T is transmittivity between the two crystals ($T = 0.90$), $\Delta\nu$ is the spectral matching ($\Delta\nu \sim 0.8$) and Δk is the spatial matching ($\Delta k \sim 0.6$). To enlighten the resilience of coherence of the output state, we can compare in Figure 2b the experimental data with the dotted curve which refers to \mathcal{V}^{th} and the dashed curve \mathcal{V}^{nc} which represents the visibility that

would be observed in the case of no preservation of the coherence during the amplification ($\mathcal{V}^{nc} = (4\overline{m} + 1)^{-1}$).

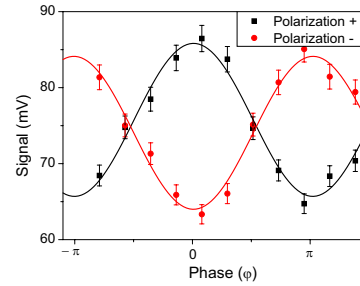


FIG. 3: Average signal versus the phase of the input qubit.

The direct correlation measurement was also carried out for a gain value equal to g_{max} : Figure 3. There the corresponding signals I_+ and I_- , averaged over 2500 triggered pulse, are reported versus the phase φ of the input qubit. The overall number of photons is equal to $M \sim 4000$ while the rescaled visibility of the fringe pattern is found: $\mathcal{V} = (19.4 \pm 1.8)\%$. These coherence patterns are the main experimental result of the present article as it shows how a *single photon quantum superposition state* coherently drives a field with large number of photons. Very important, the interference fringe patterns given in Figure 3 have been experimentally observed for all orthogonal bases belonging to the equatorial plane of the Bloch sphere of Fig.1 e.g., $\{\vec{\pi}_R = 2^{-\frac{1}{2}}(\vec{\pi}_H - i\vec{\pi}_V), \vec{\pi}_L = \vec{\pi}_R^\perp\}$ confirming the coherence between $|\Phi^H\rangle$ and $|\Phi^V\rangle$.

We address now the problem of the distinguishability between $|\Phi\rangle^\varphi$ and $|\Phi\rangle^{\varphi\perp}$, which are mutually orthogonal as shown by Equation 2, e.g., $|\Phi\rangle^\pm$. A perfect discrimination between these two states can be achieved in principle in a single run experiment by checking whether the number of photons over the \mathbf{k}_1 mode with polarization $\vec{\pi}_+$ is even or odd. Such measurement corresponds to estimating the operator $s_z = \sum_{n=0}^{\infty} [|2n+1\rangle\langle 2n+1| - |2n\rangle\langle 2n|]$ over the field k_1 with polarization $\vec{\pi}_+$. Indeed is: $s_z^{1+}|\Phi^\pm\rangle = \pm|\Phi^\pm\rangle$. The exact implementation of the operator s_z^{1+} requires a photon-number resolving detection of a mesoscopic field \mathbf{k}_1 , i.e. made up by thousands of photons. This is indeed well beyond the range of possibilities offered by the present technology [21]. Hence we could ask whether the need for such extremely fine-grained resolution could be bypassed by adopting a different approach. Let us report in Figure 4 the 3-dimensional representations of the two probability distributions of the number of photons which are associated with the two states $|\Phi\rangle^\pm$. These distributions are drawn as functions of the variables m and n which are proportional to the size of the electronic signals I_+ and I_- simultaneously registered, in any single-shot experiment, by the detectors P_+ and P_- , respectively. Precisely, $I_+ \propto m \simeq 2i$, $I_- \propto n \simeq 2j$, according to

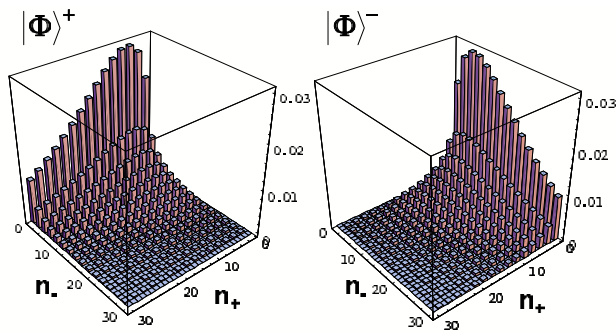


FIG. 4: Theoretical distribution probability of (n_+, n_-) for $|\Phi\rangle^\pm$ ($g = 1.6$).

Equation 2. Let us refer to $\prod^\pm(m, n)$ as the probability that a single-shot measurement $(I_+, I_-) = (m, n)$ is actually due to a realization of the state $|\Phi\rangle^\pm$. Since by Eq. 2 is found $\prod^+(m, n)/\prod^-(m, n) = m/n \equiv h$ for $2i \gg 1$ and $2j \gg 1$, we may conclude that the measured signal (I_+, I_-) can be attributed to the realization of the state $|\Phi\rangle^+$ or to $|\Phi\rangle^-$ if the measured quantity $h = I_+/I_- = m/n$ is $h \gg 1$ or $h \ll 1$, respectively. In this way we can exploit the *macroscopic character* of the output field, a continuous variable system, by a simple photon detection technique. By finding an appropriate *filtering function* $W(m, n)$, viz a weighting function of the output data (I_+, I_-) , the visibility of the detected fringe pattern can be raised to a value close to 1.

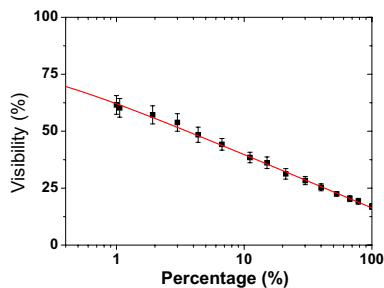


FIG. 5: Visibility of the intensity versus the percentage of data which has not been discarded within the filtering procedure. The solid line reports the best fit with the function $f(x) = a - b \ln(x+c)$. The percentage of discarded data scales $\simeq e^{-q}$.

Let us now implement experimentally the *filtering technique*. In order to do that in a sensible way we should consider two sources of errors: (1) The limited detection efficiency $\eta \ll 1$. However this effect may smooth the probability distributions $\prod^\pm(m, n)$ with no significant effect on the ratio h . (2) The spontaneous emission contribution added to the "stimulated" one. A discrimination between these latter contributions is obtained by selecting output data with large $(I_+ + I_-)$, which are most likely generated in the stimulated regime. In our single-

shot experiment we discarded the data with $|m - n| < q$ for different values of q . Of course, since any such selection reduces the rate of measurement, a convenient trading off was found necessary. Figure 5 reports the visibilities of the fringe patterns obtained by filtering the experimental data related to Figure 3 versus the percentage of registered data. The behavior is found in agreement with a refined theoretical filtering model. Interestingly, by the visibility values it is possible to demonstrate the quantum character of the mesoscopic output field. Indeed if the coherence of a general input qubit was not preserved during the amplification, the process could be described as a classical channel. Consequently the fidelity of the overall transformation would be, at most, equal to the optimal estimation fidelity for equatorial qubits: $F_{est} = \frac{3}{4}$ [15, 22]. Fig.5 achieves fidelity values above the classical threshold value: $F = \frac{(1+V)}{2} > F_{est}$ confirming the quantum character of the process. The same visibility have been observed for different pairs of input equatorial qubit, as said. The ability to discriminate the output $\{|\Phi\rangle^\varphi, |\Phi\rangle^{\varphi\perp}\}$ by the above technique opens interesting perspectives for testing quantum nonlocality in the "macroscopic" regime, such as a verification of the Bell's theorem.

In summary, we have demonstrated the interference properties of the output state in agreement with the quantum theoretical results. We reported the experimental realization of a quantum cloning machine within two new scenarios: (a) the optimal phase-covariant cloning based on the process of stimulated emission, (b) the very large number of clones $M = 4000 \gg 1$. The present work represents the first step toward an experimental interface between single qubit systems and continuous variable ones. The attempt to shed light on the quantum-to-classical transition by distributing the information from a single quantum system to many ones deserves further investigation. This work was supported by the PRIN 2005 of MIUR and project INNESCO of CNISM.

Note added in proof- Owing to experimental improvements of the pumping laser power, the following parameters have been attained: $g \simeq 5.7$, $\bar{m} \simeq 23000$.

-
- [1] V. Scarani, *et al.*, Rev. Mod. Phys. **77**, 1225 (2005).
 - [2] N.J. Cerf, *et al.*, Progress in Optics **49**, 455 (2006).
 - [3] F. De Martini, *et al.*, Prog. in Quantum Electronics **29**, 165 (2005).
 - [4] W.H. Zurek, Rev. Mod. Phys. **75**, 715 (2003); M. Schlosshauer, Rev. Mod. Phys. **76**, 1267 (2005).
 - [5] G. Chiribella, *et al.*, Phys. Rev. Lett. **97**, 250503 (2006).
 - [6] F. De Martini, Phys. Rev. Lett. **81**, 2842 (1998).
 - [7] C. Simon, *et al.*, Phys. Rev. Lett. **84**, 2993 (2000); F. De Martini *et al.*, Optics Comm. **179**, 581 (2000).
 - [8] F. De Martini, *et al.*, Nature (London) **419**, 815 (2002).
 - [9] A. Lamas-Linares, *et al.*, Science **296**, 712 (2002).

- [10] D. Pelliccia, *et al.*, Phys. Rev. A **68**, 042306 (2003); F. De Martini, *et al.*, Phys. Rev. Lett. **92**, 067901 (2004).
- [11] F. De Martini, *et al.*, Phys. Rev. Lett. **95**, 240401 (2005).
- [12] G.S. Agarwal, *et al.*, quant-ph/0608170.
- [13] F. De Martini, Phys. Lett. A **250**,15 (1998).
- [14] F. Sciarrino, *et al.*, Phys. Rev. A **72**, 062313 (2005).
- [15] D. Bruss, *et al.*, Phys. Rev. A **62**, 012302 (2000); G.M. D'Ariano, *et al.*, Phys. Rev. A **64**, 042308 (2001).
- [16] D. Bruss, *et al.*, J. Phys. A **34**, 6815 (2001).
- [17] E. Schroedinger, Naturwissenschaften 23, 807 (1935).
- [18] W. Schleich, Quantum Optics in Phase Space (Wiley, New York 2001).
- [19] H.S. Eisenberg, *et al.*, Phys. Rev. Lett. **93**, 019301 (2004).
- [20] M. Caminati, *et al.*, Phys. Rev. A **73**, 032312 (2006); *ibid*, **74**, 062304 (2006).
- [21] S. Portolan, *et al.*, Phys. Rev. A **73**, 020102 (2006).
- [22] The bound $F_{est} = \frac{3}{4}$ for equatorial qubits holds also for probabilistic estimation measurements.